

**Field theory of bicritical and tetracritical points. I. Statics**R. Folk,<sup>1,\*</sup> Yu. Holovatch,<sup>2,1,†</sup> and G. Moser<sup>3,‡</sup><sup>1</sup>*Institute for Theoretical Physics, Johannes Kepler University Linz, Altenbergerstrasse 69, A-4040, Linz, Austria*<sup>2</sup>*Institute for Condensed Matter Physics, National Academy of Sciences of Ukraine, 1 Svientsitskii Street, UA-79011 Lviv, Ukraine*<sup>3</sup>*Department for Material Research and Physics, Paris Lodron University Salzburg, Hellbrunnerstrasse 34, A-5020 Salzburg, Austria*

(Received 6 June 2008; published 28 October 2008)

We calculate the static critical behavior of systems of  $O(n_{\parallel}) \oplus O(n_{\perp})$  symmetry by the renormalization group method within the minimal subtraction scheme in two-loop order. Summation methods lead to fixed points describing multicritical behavior. Their stability border lines in the space of the order parameter components  $n_{\parallel}$  and  $n_{\perp}$  and spatial dimension  $d$  are calculated. The essential features obtained already in two-loop order for the interesting case of an antiferromagnet in a magnetic field ( $n_{\parallel}=1$ ,  $n_{\perp}=2$ ) are the stability of the biconical fixed point and the neighborhood of the stability border lines to the other fixed points, leading to very small transient exponents. We are also able to calculate the flow of static couplings, which allows us to consider the attraction region. Depending on the nonuniversal background parameters, the existence of different multicritical behavior (bicritical or tetracritical) is possible, including a triple point.

DOI: [10.1103/PhysRevE.78.041124](https://doi.org/10.1103/PhysRevE.78.041124)

PACS number(s): 05.50.+q, 64.60.ae

**I. INTRODUCTION**

Antiferromagnets in an external magnetic field show a variety of phase diagrams depending on the interaction terms present in the spin Hamiltonian [1]. The spin interaction may be isotropic, or anisotropic with an easy axis and/or single-ion anisotropy terms, where the anisotropy is in the direction of the external magnetic field. The phase diagrams of such models exhibit a multicritical point, where several transition lines meet.

At a *bicritical* point three phases—an antiferromagnetic phase, a spin flop phase and the paramagnetic phase—are in coexistence. The phase transition lines to the paramagnetic phase are second-order transition lines, whereas the transition line between the spin flop and the antiferromagnetic phases is of first order. At the *tetracritical* point four phases—an antiferromagnetic phase, a spin flop phase, an intermediate or mixed phase, and the paramagnetic phase—are in coexistence. All transition lines are of second order in this case.

A field theoretic description of these models starts with a static functional for an  $n$ -component field  $\Phi$  of  $O(n_{\parallel}) \oplus O(n_{\perp})$  symmetry ( $n_{\parallel}+n_{\perp}=n$ ) leading to different multicritical behavior connected with the stable fixed point (FP) found in the renormalization group treatment [2–4]. Bicritical behavior has been connected with the stability of the well-known *isotropic Heisenberg* fixed point of  $O(n_{\parallel}+n_{\perp})$  symmetry, whereas tetracriticality has been connected with a fixed point of  $O(n_{\parallel}) \oplus O(n_{\perp})$  symmetry, which might be either the so-called *biconical* FP or the *decoupling* FP. In the last FP the parallel and the perpendicular components of the order parameter (OP) are asymptotically decoupled.

The important questions that theory should give an answer to are the following. (i) Which of these FPs is the stable

one in a three- or two-dimensional system, and (ii) what are the differences in the critical behavior at the multicritical point? These questions have been raised and considered in one-loop order [4], where the Heisenberg FP turns out to be the stable one in  $d=3$  for the case  $n_{\parallel}=1$  and  $n_{\perp}=2$ , but this picture is changed in higher-loop order. In a five-loop order  $\varepsilon=4-d$  expansion, it has been found that the biconical FP is the stable one [5]. It also has been found that the differences between the exponents at the different multicritical points are much smaller than in the one-loop order calculation.

Physical examples where such multicritical behavior has been found are the anisotropic antiferromagnets [6] (with the magnetic field in the hard direction) like  $\text{GdAlO}_3$  [7,8] and [9]  $\text{MnF}_2$  [9], as well as  $\text{MnCl}_2\text{4D}_2\text{O}$  [10] or  $\text{Mn}_2\text{As}_4$  ( $A=\text{Si}$  or  $\text{Ge}$ ) [11]. Other examples with a single-ion anisotropy might be layered cuprate antiferromagnets like  $(\text{Ca,La})_{14}\text{Cu}_{24}\text{O}_{41}$ . Besides the examples with  $n_{\parallel}=1$  and  $n_{\perp}=2$  one might consider other cases:  $n_{\parallel}=1$  and  $n_{\perp}=1$  when additional anisotropies are present as in  $\text{NiCl}_2$  [12,13] or high- $T_c$  superconductors representing a system with  $n_{\parallel}=2$  (corresponding to the superconductor OP) and  $n_{\perp}=3$  (corresponding to the antiferromagnetic OP).

Quite recently the possible types of phase diagrams in the magnetic field–temperature plane of a  $d=3$  uniaxially anisotropic antiferromagnet have been studied by Monte Carlo simulations [14,15]. For  $n_{\parallel}=1$  and  $n_{\perp}=2$ , a phase diagram with a bicritical point has been found in agreement with earlier simulations [16], but contrary to the results of renormalization group theory in higher-loop orders [5].

A general picture is obtained when one considers a generalized model with an  $n$ -component order parameter, which splits into  $n_{\parallel}$  parallel OP components and  $n_{\perp}$  perpendicular OP components and quartic interaction terms of  $O(n_{\parallel}) \oplus O(n_{\perp})$  symmetry. Both parallel and perpendicular OP components become critical at the multicritical point. In the  $n_{\parallel}-n_{\perp}$  space regions of different types of multicriticality exist touching each other at stability border lines (“phase border lines”) where the fixed points change their stability (such a picture of the different stability regions might be called a “phase diagram”). In addition to the stability of a fixed point,

\*folk@tphys.uni-linz.ac.at

†hol@icmp.lviv.ua

‡guenter.moser@sbg.ac.at

we want to mention that one has to consider also the attraction regions of a fixed point to answer the question of whether one can reach the stable fixed point. In order to discuss the attraction regions, one has to consider the flow of the couplings from the nonuniversal initial (background) values.

We therefore reconsider the critical behavior of systems with  $O(n_{\parallel}) \oplus O(n_{\perp})$  symmetry. Being interested in criticality of three-dimensional systems, we will work within the minimal subtraction scheme and evaluate the results at fixed dimension  $d=3$  [17]. For the universal properties (such as asymptotic critical exponents and marginal dimensions), it turns out that already the two-loop calculations refined by resummation are in good quantitative agreement with previous resummed higher-order  $\varepsilon$  expansion results [5]. However, contrary to previous calculations, the technique we use gives the possibility of analyzing nonuniversal effective critical behavior which is manifested in a broader temperature interval near the (multi)critical point. Such calculations are out of reach the  $\varepsilon$  expansion and will be performed below on the base of analysis of the renormalization group flow.

The paper is organized as follows. Starting from the static functional (Sec. II), we introduce the renormalization in Sec. III and calculate the field theoretic functions in Sec. IV. The perturbative expansions being asymptotic, we apply in Sec. V the resummation technique to restore their convergence and to extract numerical values of the fixed points of the renormalization group transformations and their stability. We discuss the stability border lines between the fixed points and show that they are shifted considerably compared to the one-loop calculation. As a result, for the isotropic antiferromagnet in a magnetic field represented by the point (1,2) in the  $n_{\parallel}-n_{\perp}$  space, the biconical fixed point is stable, predicting tetracritical behavior if the fixed point is reached from the background. The very neighborhood of the stability border lines is characterized by very small transient exponents. Moreover, looking at the attraction regions, a surface in the space of the fourth-order couplings exists above which no finite fixed point can be reached. This indicates the possibility of a scenario mentioned already earlier [5,18,19], where the multicritical point is a triple point and the second-order lines separating the paramagnetic phase from the ordered phases contain a tricritical point. In Sec. VI the critical exponents are defined and their asymptotic values are calculated for the physically interesting case  $n_{\parallel}=1$ ,  $n_{\perp}=2$ . The flow equations and effective exponents are discussed in Sec. VII, leading to our final conclusions and outlook in Sec. VIII. In the appendixes we discuss the perturbative expansion for the vertex functions (Appendix A) and explain the resummation procedure exploited in our calculations (Appendix B).

## II. STATIC FUNCTIONAL

The critical behavior of an isotropic system [ $O(n)$  symmetry] with short-range interaction is determined by the static functional

$$\mathcal{H}_{\text{GLW}} = \int d^d x \left( \frac{1}{2} \dot{r} \vec{\phi}_0 \cdot \vec{\phi}_0 + \frac{1}{2} \sum_{i=1}^n \nabla_i \vec{\phi}_0 \cdot \nabla_i \vec{\phi}_0 + \frac{\dot{u}}{4!} (\vec{\phi}_0 \cdot \vec{\phi}_0)^2 \right), \quad (1)$$

which is known as the Ginzburg-Landau-Wilson (GLW) functional. The order parameter  $\vec{\phi}_0 \equiv \vec{\phi}_0(x)$  is assumed to be an  $n$ -component real vector. The centered dot denotes the scalar product between vectors.  $\dot{r}$  is proportional to the temperature distance to the critical point and  $\dot{u}$  is the fourth-order coupling in which perturbation expansion is usually performed. Systems represented by such a static functional have been extensively studied in the last decades with different renormalization procedures, and the corresponding critical exponents and amplitude ratios are known up to high loop orders (see, e.g., [20]).

In order to describe bicritical behavior, the  $n$ -dimensional space of the order parameter components will be divided into two subspaces with dimensions  $n_{\perp}$  and  $n_{\parallel}$  with the property  $n_{\perp} + n_{\parallel} = n$  in the following. Correspondingly, the order parameter separates into

$$\vec{\phi}_0 = \begin{pmatrix} \vec{\phi}_{\perp 0} \\ \vec{\phi}_{\parallel 0} \end{pmatrix}, \quad (2)$$

where  $\vec{\phi}_{\perp 0}$  is the  $n_{\perp}$ -dimensional order parameter of the  $n_{\perp}$  subspace, and  $\vec{\phi}_{\parallel 0}$  is the  $n_{\parallel}$ -dimensional order parameter of the  $n_{\parallel}$  subspace. Performing the separation in the GLW functional (1), one obtains

$$\begin{aligned} \mathcal{H}_{\text{bi}} = \int d^d x & \left( \frac{1}{2} \dot{r}_{\perp} \vec{\phi}_{\perp 0} \cdot \vec{\phi}_{\perp 0} + \frac{1}{2} \sum_{i=1}^{n_{\perp}} \nabla_i \vec{\phi}_{\perp 0} \cdot \nabla_i \vec{\phi}_{\perp 0} \right. \\ & + \frac{1}{2} \dot{r}_{\parallel} \vec{\phi}_{\parallel 0} \cdot \vec{\phi}_{\parallel 0} + \frac{1}{2} \sum_{i=1}^{n_{\parallel}} \nabla_i \vec{\phi}_{\parallel 0} \cdot \nabla_i \vec{\phi}_{\parallel 0} + \frac{\dot{u}_{\perp}}{4!} (\vec{\phi}_{\perp 0} \cdot \vec{\phi}_{\perp 0})^2 \\ & \left. + \frac{\dot{u}_{\parallel}}{4!} (\vec{\phi}_{\parallel 0} \cdot \vec{\phi}_{\parallel 0})^2 + \frac{2\dot{u}_{\times}}{4!} (\vec{\phi}_{\perp 0} \cdot \vec{\phi}_{\perp 0})(\vec{\phi}_{\parallel 0} \cdot \vec{\phi}_{\parallel 0}) \right). \quad (3) \end{aligned}$$

This functional contains three fourth-order couplings  $\{\dot{u}\} = \{\dot{u}_{\perp}, \dot{u}_{\times}, \dot{u}_{\parallel}\}$  and, instead of one parameter  $\dot{r}$  as in (1), in (3) two different parameters  $\dot{r}_{\perp}$  and  $\dot{r}_{\parallel}$  appear referring to different temperature distances.

The decomposition into parallel and perpendicular OP components allows us to describe the critical behavior at the meeting point of two critical lines: (i) the line where  $\dot{r}_{\perp}$  becomes zero and the  $n_{\perp}$ -dimensional components  $\vec{\phi}_{\perp 0}$  are the OP, and (ii) the line where  $\dot{r}_{\parallel}$  becomes zero and the  $n_{\parallel}$ -dimensional components  $\vec{\phi}_{\parallel 0}$  are the OP. At the meeting point, both quadratic terms become zero and both components of  $\vec{\phi}_0$  have to be taken into account. The critical behavior of this multicritical point has been described already in one-loop order [4], and three different types of multicritical behavior have been found; (i) one described by the well-known isotropic  $n$ -component Heisenberg fixed point where all fourth-order couplings are equal, (ii) one described by a

decoupling fixed point, which consists of a combination of two  $n_{\perp}$  and  $n_{\parallel}$  component isotropic Heisenberg fixed points of two decoupled systems, and (iii) a new type of fixed point called the biconical fixed point. Which of these fixed points is the stable one depends on the number of components  $n_{\perp}$  and  $n_{\parallel}$  and the dimension  $d$  of space. The scaling properties depend on the symmetry of stable fixed point. When the  $O(n)$  symmetry in the OP space is broken to  $O(n_{\parallel}) \oplus O(n_{\perp})$  symmetry, then also the spatial correlations are different for the two OP subspaces.

### III. RENORMALIZATION

The procedure used to obtain the vertex functions appropriate for the renormalization is described in more details in Appendix A. From the general structure of the two-point vertex functions presented therein, it follows that the order parameter functions  $\vec{\phi}_{\perp 0}$  and  $\vec{\phi}_{\parallel 0}$  in the subspaces may be renormalized by the scalar renormalization factors

$$\vec{\phi}_{\perp 0} = Z_{\phi_{\perp}}^{1/2} \vec{\phi}_{\perp}, \quad \vec{\phi}_{\parallel 0} = Z_{\phi_{\parallel}}^{1/2} \vec{\phi}_{\parallel}. \quad (4)$$

The above relations and the definitions (A7) and (A8) imply that the correlation lengths  $\xi_{\parallel}$  and  $\xi_{\perp}$  do not renormalize. They constitute together with the wave vector modulus  $k$  the independent lengths of the system. The fourth-order couplings may also be renormalized by scalar renormalization factors

$$\hat{u}_{\perp} = \kappa^{\varepsilon} Z_{\phi_{\perp}}^{-2} Z_{u_{\perp}} u_{\perp} A_d^{-1}, \quad (5)$$

$$\hat{u}_{\times} = \kappa^{\varepsilon} Z_{\phi_{\perp}}^{-1} Z_{\phi_{\parallel}}^{-1} Z_{u_{\times}} u_{\times} A_d^{-1}, \quad (6)$$

$$\hat{u}_{\parallel} = \kappa^{\varepsilon} Z_{\phi_{\parallel}}^{-2} Z_{u_{\parallel}} u_{\parallel} A_d^{-1}, \quad (7)$$

with the geometrical factor

$$A_d = \Gamma\left(1 - \frac{\varepsilon}{2}\right) \Gamma\left(1 + \frac{\varepsilon}{2}\right) \frac{\Omega_d}{(2\pi)^d}, \quad (8)$$

analogously to Dohm [21]. In (8)  $\Gamma(x)$  denotes the Euler Gamma function and  $\Omega_d$  is the surface of the  $d$ -dimensional unit sphere.  $\kappa$  is the usual reference wave vector modulus representing a scaling parameter. We want to remark that it would be possible to introduce a  $3 \times 3$  matrix for the renormalization of the three fourth-order couplings  $\{\hat{u}\}$  as performed in [5]. The resulting  $\beta$  functions are the same anyway. Thus it remains a matter of taste if one uses a scalar or a matrix renormalization for the three fourth-order couplings. The situation changes if one considers  $\phi^2$  insertions. The vertex function  $\Gamma_{\perp\perp\perp}^{(2,1)}$  splits up into four functions  $\Gamma_{\perp\perp\perp}^{(2,1)}$ ,  $\Gamma_{\perp\perp\parallel}^{(2,1)}$ ,  $\Gamma_{\parallel\parallel\parallel}^{(2,1)}$ , and  $\Gamma_{\parallel\parallel\perp}^{(2,1)}$  (for the notation see Appendix A). A consistent renormalization of the  $\phi^2$  insertions is possible only by the introduction of

$$\begin{pmatrix} \vec{\phi}_{\perp}^2 \\ \vec{\phi}_{\parallel}^2 \end{pmatrix} = \mathbf{Z}_{\phi^2} \begin{pmatrix} \vec{\phi}_{\perp 0}^2 \\ \vec{\phi}_{\parallel 0}^2 \end{pmatrix} \quad (9)$$

with the renormalization matrix

$$\mathbf{Z}_{\phi^2} = \begin{pmatrix} Z_{11} & Y_{12} \\ Y_{21} & Z_{22} \end{pmatrix}. \quad (10)$$

The zeroth order of the perturbation expansion appears only in the diagonal elements  $Z_{ii} = 1 + O(\{u\})$ , while the off-diagonal elements  $Y_{ij} = O(\{u\})$  start with the one-loop order. With (4) and (9) an arbitrary vertex function (A9) renormalizes as

$$\begin{aligned} \Gamma_{\alpha_1 \dots \alpha_N; \beta_1 \dots \beta_L}^{(N,L)} &= Z_{\phi_{\alpha_1}}^{1/2} \dots Z_{\phi_{\alpha_N}}^{1/2} \\ &\times \sum_{i_1, \dots, i_L} (\mathbf{Z}_{\phi^2})_{\beta_1 i_1} \dots (\mathbf{Z}_{\phi^2})_{\beta_L i_L} \Gamma_{\alpha_1 \dots \alpha_N; i_1 \dots i_L}^{(N,L)}. \end{aligned} \quad (11)$$

The indices  $\alpha_j$ ,  $\beta_j$ , and  $i_j$  are running over  $\perp$  and  $\parallel$ . The renormalization introduced in the above relations removes the poles from all vertex functions except the functions  $\Gamma_{\beta_1 \beta_2}^{(0,2)}$ , which have to be considered separately. Thus Eq. (11) is valid for all vertex functions except  $\Gamma_{\beta_1 \beta_2}^{(0,2)}$ . The multiplicative renormalization in (11) does not remove all singularities at  $d=4$  in these functions. In order to remove the remaining poles, an additional additive renormalization is necessary. The multiplicative renormalization leads to functions

$$\Gamma_{R; \beta_1 \beta_2}^{(0,2)} = \sum_{i_1, i_2} (\mathbf{Z}_{\phi^2})_{\beta_1 i_1} (\mathbf{Z}_{\phi^2})_{\beta_2 i_2} \Gamma_{i_1 i_2}^{(0,2)}. \quad (12)$$

A finite function can be obtained by subtracting the singular part  $[\Gamma_{R; \beta_1 \beta_2}^{(0,2)}]_S$  from (12). Thus we may introduce

$$\Gamma_{\beta_1 \beta_2}^{(0,2)} = \kappa^{\varepsilon} A_d^{-1} (\Gamma_{R; \beta_1 \beta_2}^{(0,2)} - [\Gamma_{R; \beta_1 \beta_2}^{(0,2)}]_S) \quad (13)$$

as renormalized functions. The additive renormalizations are then defined by

$$A_{\beta_1 \beta_2}(\{u\}) = \kappa^{\varepsilon} A_d^{-1} [\Gamma_{R; \beta_1 \beta_2}^{(0,2)}]_S. \quad (14)$$

The three functions  $A_{\perp\perp}$ ,  $A_{\parallel\parallel}$ , and  $A_{\perp\parallel} = A_{\parallel\perp}$  in (14) represent the extension of the function  $A(u)$  in the isotropic case [22] and may be written as the symmetric matrix

$$\mathbf{A}(\{u\}) = \begin{pmatrix} A_{\perp\perp} & A_{\perp\parallel} \\ A_{\perp\parallel} & A_{\parallel\parallel} \end{pmatrix}. \quad (15)$$

Within statics it may also be convenient to work with the temperature-dependent vertex functions without introducing the correlation length, as described in Appendix A at stage (A6). This allows us to avoid functions with  $\phi^2$  insertions except for the specific heat. In this case a renormalization for the temperature distances  $\Delta_{\perp}^{\circ}$  and  $\Delta_{\parallel}^{\circ}$  has to be introduced as performed in [21]. In order to obtain renormalization factors which do not contain ratios of the temperature distances, a matrix renormalization

$$\Delta \hat{r}^{\circ} \equiv \begin{pmatrix} \Delta_{\perp}^{\circ} \\ \Delta_{\parallel}^{\circ} \end{pmatrix} = \mathbf{Z}_{\phi}^{-1} \cdot \mathbf{Z}_r \cdot \Delta \hat{r} \quad (16)$$

with the matrices

$$\mathbf{Z}_r = \begin{pmatrix} Z_{r\perp} & Y_{r\perp} \\ Y_{r\parallel} & Z_{r\parallel} \end{pmatrix}, \quad \mathbf{Z}_\phi = \begin{pmatrix} Z_{\phi\perp} & 0 \\ 0 & Z_{\phi\parallel} \end{pmatrix} \quad (17)$$

has to be used. The renormalization factors in the matrix above are obtained by collecting the  $\varepsilon$ -poles proportional to  $\Delta r_\perp$  and  $\Delta r_\parallel$  in the two vertex functions  $\Gamma_{\perp\perp}^{\circ(2,0)}$  and  $\Gamma_{\parallel\parallel}^{\circ(2,0)}$ . The matrices in (17) are related to the renormalization matrix  $\mathbf{Z}_{\phi^2}$  for the  $\phi^2$  insertions by

$$\mathbf{Z}_{\phi^2} = (\mathbf{Z}_\phi^{-1} \cdot \mathbf{Z}_r)^T = \mathbf{Z}_r^T \cdot \mathbf{Z}_\phi^{-1}, \quad (18)$$

which represents the matrix counterpart of the scalar relation in the isotropic case. The superscript  $T$  denotes the transposed matrix.

#### IV. $\zeta$ AND $\beta$ FUNCTIONS

From the scalar renormalization factors  $Z_{\phi_{\alpha_i}}$  ( $\alpha_i = \perp, \parallel$ ) the  $\zeta$  functions

$$\zeta_{\phi_{\alpha_i}}(\{u\}) = \frac{d \ln Z_{\phi_{\alpha_i}}^{-1}}{d \ln \kappa} \quad (19)$$

are derived. The  $\kappa$  derivatives, as also in the following definitions, always are taken at fixed unrenormalized parameters. In two-loop order we obtain the  $\zeta$  functions

$$\zeta_{\phi\perp} = -\frac{n_\perp + 2}{72} u_\perp^2 - \frac{n_\parallel}{72} u_\times^2, \quad (20)$$

$$\zeta_{\phi\parallel} = -\frac{n_\perp}{72} u_\times^2 - \frac{n_\parallel + 2}{72} u_\parallel^2. \quad (21)$$

From the matrix  $\mathbf{Z}_{\phi^2}$  of the renormalization of the  $\phi^2$  insertions, it is convenient to introduce the  $\zeta$  matrix

$$[\zeta_{\phi^2}]_{ij}(\{u\}) = -\sum_l \left( \kappa \frac{d}{d\kappa} [\mathbf{Z}_{\phi^2}]_{il} \right) [\mathbf{Z}_{\phi^2}^{-1}]_{lj}. \quad (22)$$

A matrix  $\zeta_r$  following from  $\mathbf{Z}_r$ , which has been defined in (17), also can be introduced, analogously to (22), by replacing  $\mathbf{Z}_{\phi^2}$  with  $\mathbf{Z}_r$ . In two-loop order the components of the matrix  $\zeta_{\phi^2}$  are

$$[\zeta_{\phi^2}]_{11} = \frac{n_\perp + 2}{6} u_\perp \left( 1 - \frac{5}{12} u_\perp \right) - \frac{n_\parallel}{72} u_\times^2, \quad (23)$$

$$[\zeta_{\phi^2}]_{12} = \frac{n_\perp}{6} u_\times \left( 1 - \frac{u_\times}{3} \right), \quad (24)$$

$$[\zeta_{\phi^2}]_{21} = \frac{n_\parallel}{6} u_\times \left( 1 - \frac{u_\times}{3} \right), \quad (25)$$

$$[\zeta_{\phi^2}]_{22} = \frac{n_\parallel + 2}{6} u_\parallel \left( 1 - \frac{5}{12} u_\parallel \right) - \frac{n_\perp}{72} u_\times^2. \quad (26)$$

The nondiagonal elements (24) and (25) are proportional to  $u_\times$  and differ only in a prefactor  $n_\perp$  and  $n_\parallel$ , respectively. Thus we may write

$$[\zeta_{\phi^2}]_{12} = \frac{1}{6} n_\perp u_\times C(\{u\}) = \frac{n_\perp}{n_\parallel} [\zeta_{\phi^2}]_{21} \quad (27)$$

with a function

$$C(\{u\}) = \left( 1 - \frac{u_\times}{3} \right) \quad (28)$$

in two-loop order. Relation (18) between  $\mathbf{Z}_{\phi^2}$  and  $\mathbf{Z}_r$  implies

$$\zeta_{\phi^2}^T = \zeta_r - \zeta_\phi, \quad (29)$$

where the diagonal matrix  $\zeta_\phi = \text{diag}(\zeta_{\phi\perp}, \zeta_{\phi\parallel})$  has been introduced. From the additive renormalization (15), the function

$$\begin{aligned} [\mathbf{B}_{\phi^2}]_{ij}(\{u\}) &= \kappa^\varepsilon \sum_{n,p} [\mathbf{Z}_{\phi^2}]_{in} [\mathbf{Z}_{\phi^2}]_{jp} \sum_{l,m} \kappa \frac{d}{d\kappa} \kappa^{-\varepsilon} \\ &\times [\mathbf{Z}_{\phi^2}^{-1}]_{nl} [\mathbf{Z}_{\phi^2}^{-1}]_{pm} [\mathbf{A}]_{lm}(\{u\}) \end{aligned} \quad (30)$$

can be introduced, which is the extension of the scalar function  $B_{\phi^2}(u)$  in the isotropic case (see Ref. [22] for definitions). Calculating (30) in two-loop order, we obtain

$$\mathbf{B}_{\phi^2}(\{u\}) = \begin{pmatrix} n_\perp/2 & 0 \\ 0 & n_\parallel/2 \end{pmatrix} + O(\{u^2\}). \quad (31)$$

The  $\beta$  functions of the four couplings are defined as

$$\beta_{u_a}(\{u\}) = \kappa \frac{du_a}{d\kappa} \quad (32)$$

with  $a = \perp, \parallel, \times$ . In two-loop order the explicit expressions of the  $\beta$  functions are

$$\begin{aligned} \beta_{u_\perp} &= -\varepsilon u_\perp + \frac{(n_\perp + 8)}{6} u_\perp^2 + \frac{n_\parallel}{6} u_\times^2 - \frac{(3n_\perp + 14)}{12} u_\perp^3 \\ &\quad - \frac{5n_\parallel}{36} u_\perp u_\times^2 - \frac{n_\parallel}{9} u_\times^3, \end{aligned} \quad (33)$$

$$\begin{aligned} \beta_{u_\times} &= -\varepsilon u_\times + \frac{(n_\perp + 2)}{6} u_\perp u_\times + \frac{(n_\parallel + 2)}{6} u_\times u_\parallel + \frac{2}{3} u_\times^2 \\ &\quad - \frac{(n_\perp + n_\parallel + 16)}{72} u_\times^3 - \frac{(n_\perp + 2)}{6} u_\times^2 u_\perp - \frac{(n_\parallel + 2)}{6} u_\times^2 u_\parallel \\ &\quad - \frac{5(n_\perp + 2)}{72} u_\perp^2 u_\times - \frac{5(n_\parallel + 2)}{72} u_\times u_\parallel^2, \end{aligned} \quad (34)$$

$$\begin{aligned} \beta_{u_\parallel} &= -\varepsilon u_\parallel + \frac{(n_\parallel + 8)}{6} u_\parallel^2 + \frac{n_\perp}{6} u_\times^2 - \frac{(3n_\parallel + 14)}{12} u_\parallel^3 - \frac{5n_\perp}{36} u_\parallel u_\times^2 \\ &\quad - \frac{n_\perp}{9} u_\times^3. \end{aligned} \quad (35)$$

The flow equations of the fourth-order couplings  $u_a$  are

$$l \frac{du_a}{dl} = \beta_{u_a}(\{u\}) \quad (36)$$

where  $l$  is the flow parameter.



TABLE I. Fixed points and stability exponents of the  $O(n_{\parallel}) \oplus O(n_{\perp})$  model.

FP	$u_{\perp}^*$	$u_{\times}^*$	$u_{\parallel}^*$	$\omega_1$	$\omega_2$	$\omega_3$
$\mathcal{G}$	0	0	0	$-\varepsilon$	$-\varepsilon$	$-\varepsilon$
$\mathcal{H}(n_{\perp})$	$u^{\mathcal{H}(n_{\perp})}$	0	0	$\omega^{\mathcal{H}(n_{\perp})}$	$\omega_2^{\mathcal{H}(n_{\perp})}$	$-\varepsilon$
$\mathcal{H}(n_{\parallel})$	0	0	$u^{\mathcal{H}(n_{\parallel})}$	$-\varepsilon$	$\omega_2^{\mathcal{H}(n_{\parallel})}$	$\omega^{\mathcal{H}(n_{\parallel})}$
$\mathcal{D}$	$u^{\mathcal{H}(n_{\perp})}$	0	$u^{\mathcal{H}(n_{\parallel})}$	$\omega^{\mathcal{H}(n_{\perp})}$	$\omega_2^{\mathcal{D}}$	$\omega^{\mathcal{H}(n_{\parallel})}$
$\mathcal{H}(n_{\perp} + n_{\parallel})$	$u^{\mathcal{H}(n_{\perp} + n_{\parallel})}$	$u^{\mathcal{H}(n_{\perp} + n_{\parallel})}$	$u^{\mathcal{H}(n_{\perp} + n_{\parallel})}$	$\omega_1^{\mathcal{H}(n_{\perp} + n_{\parallel})}$	$\omega_2^{\mathcal{H}(n_{\perp} + n_{\parallel})}$	$\omega_3^{\mathcal{H}(n_{\perp} + n_{\parallel})}$
$\mathcal{B}$	$u_{\perp}^{\mathcal{B}}$	$u_{\times}^{\mathcal{B}}$	$u_{\parallel}^{\mathcal{B}}$	$\omega_1^{\mathcal{B}}$	$\omega_2^{\mathcal{B}}$	$\omega_3^{\mathcal{B}}$
$\mathcal{U}_1$	$u_{\perp}^{\mathcal{U}_1}$	$u_{\times}^{\mathcal{U}_1}$	$u_{\parallel}^{\mathcal{U}_1}$	$\omega_1^{\mathcal{U}_1}$	$\omega_2^{\mathcal{U}_1}$	$\omega_3^{\mathcal{U}_1}$
$\mathcal{U}_2$	$u_{\perp}^{\mathcal{U}_2}$	$u_{\times}^{\mathcal{U}_2}$	$u_{\parallel}^{\mathcal{U}_2}$	$\omega_1^{\mathcal{U}_2}$	$\omega_2^{\mathcal{U}_2}$	$\omega_3^{\mathcal{U}_2}$

**V. FIXED POINTS AND THEIR STABILITY ('PHASE DIAGRAM')**

The FPs of the flow equations (36) are given by the solutions of the system of equations:

$$\beta_{u_a}(\{u\}) = 0. \tag{37}$$

At the one-loop order, Eq. (37) defines eight fixed points. Six of them are real and two are complex apart from the region where  $n_{\parallel}$  and  $n_{\perp}$  are small (see Table I). They all have the property of being proportional to  $\varepsilon = 4 - d$ . To proceed with higher-loop approximations, one can make use of different calculation schemes, either performing an  $\varepsilon$  expansion or solving the flow equations directly for fixed  $d = 3$  (i.e., for  $\varepsilon = 1$ ) [17]. A particular feature of the  $\varepsilon$ -expansion is that an increase of the order of approximation does not lead to an increase of the number of FPs [23]. Once the FPs are found in the first order of  $\varepsilon$ , the next orders of the expansion give only the next-order contributions to the first-order values of the FPs but do not lead to the appearance of new FPs. On the contrary, when one directly solves nonlinear flow equations for fixed  $d$  in higher-loop order, more and more fixed points may appear in addition since the order of the polynomials to be solved for the fixed points increases. Moreover, the physical FPs found in  $\varepsilon$  expansion may disappear when one naively solves the flow equations for fixed space dimension  $d$ . It is well established by now that the expansions involved for the field theoretic renormalization group functions are asymptotic at best [20] and one has to use appropriate resummation procedures to get reliable results on their basis. Let us note, however, that whereas in the  $\varepsilon$  expansion the resummation procedure is needed only to make precise the FP values, in the fixed- $d$  approach it is the resummation that allows one to judge whether a FP is present at all, and comparative analysis of the two approaches allows one to judge about the FP picture on a sound basis [24]. Below we will make use of these two approaches. We will work within the two-loop approximation and show that the two loop  $\varepsilon$  expansion is not sufficient even when one uses resummation in contrast to the fixed-dimension procedure.

Defining the FP picture we are looking for answers to the following questions. (i) Is the critical behavior described by a certain FP with corresponding asymptotic and universal critical exponents? (ii) Is the system very near a stability border line and slow transients lead to an effective and non-

universal critical behavior? In such a case the whole information contained in the nonlinear flow equations is necessary and available only in the second method presented here. Furthermore, in answering these questions we demonstrate that the *physically* relevant features are obtained already using the two-loop approximation.

**A. Results in two-loop  $\varepsilon$  expansion**

Starting from Eqs. (33)–(35) one gets six real FPs, as shown in Table I. Four fixed points correspond to the decoupled effective Hamiltonians of the  $O(n_{\perp})$  and  $O(n_{\parallel})$  models. Besides the Gaussian FP  $\mathcal{G}(u_{\perp}^* = u_{\times}^* = u_{\parallel}^* = 0)$ , these are the  $\mathcal{H}(n_{\perp})$  and  $\mathcal{H}(n_{\parallel})$  FPs with  $(u_{\perp}^* = u^{\mathcal{H}(n_{\perp})}, u_{\times}^* = u_{\parallel}^* = 0)$  and  $(u_{\parallel}^* = u^{\mathcal{H}(n_{\parallel})}, u_{\times}^* = u_{\perp}^* = 0)$ , respectively, as well as the decoupling FP  $\mathcal{D}(u_{\perp}^* = u^{\mathcal{H}(n_{\perp})}, u_{\times}^* = 0, u_{\parallel}^* = u^{\mathcal{H}(n_{\parallel})})$ . Here and below, by  $u^{\mathcal{H}(n)}$  we denote the Heisenberg FP of the  $O(n)$ -symmetrical model. Two more FPs correspond to the nonzero value of the coupling  $u_{\times}^*$ . Following the nomenclature of Ref. [4] we call them the isotropic Heisenberg and biconical FPs,  $\mathcal{H}(n_{\perp} + n_{\parallel})$  and  $\mathcal{B}$ , respectively (see Table I). In the minimal subtraction renormalization group (RG) scheme, the value of  $u^{\mathcal{H}(n)}$  is currently known at  $\varepsilon^5$  order [25]. From any of the  $\beta$  functions (33)–(35) one recovers the familiar  $\varepsilon^2$  result

$$u^{\mathcal{H}(n)} = \frac{6\varepsilon}{n+8} + \frac{18(3n+14)\varepsilon^2}{(n+8)^3}. \tag{38}$$

Expressions for the coordinates of the FP  $\mathcal{B}$  are too cumbersome to be given in a compact form for general  $n_{\parallel}$  and  $n_{\perp}$ . Below we list the nonzero values for the FP according to Table I for the physically important case  $n_{\parallel} = 1, n_{\perp} = 2$  we are interested in. Note that for this case the two FPs  $\mathcal{U}_1$  and  $\mathcal{U}_2$  are complex conjugate:

$$\begin{aligned} u_{\parallel}^{\mathcal{H}(1)} &= 0.666\ 67\varepsilon + 0.419\ 75\varepsilon^2, \\ u_{\perp}^{\mathcal{H}(2)} &= 0.600\ 00\varepsilon + 0.360\ 00\varepsilon^2, \\ u_{\parallel}^{\mathcal{H}(3)} &= 0.545\ 45\varepsilon + 0.311\ 04\varepsilon^2, \\ u_{\parallel}^{\mathcal{B}} &= 0.404\ 96\varepsilon + 0.386\ 91\varepsilon^2, \\ u_{\perp}^{\mathcal{B}} &= 0.505\ 69\varepsilon + 0.316\ 10\varepsilon^2, \end{aligned}$$

$$u_{\times}^{\mathcal{B}} = 0.690\,59\varepsilon + 0.299\,26\varepsilon^2,$$

$$u_{\parallel}^{\mathcal{U}1} = (0.415\,21 - i0.329\,36)\varepsilon + (0.212\,59 - i0.211\,59)\varepsilon^2,$$

$$u_{\perp}^{\mathcal{U}1} = (0.202\,13 + i0.124\,00)\varepsilon + (0.151\,82 + i0.7087)\varepsilon^2,$$

$$u_{\times}^{\mathcal{U}1} = (0.986\,46 + i0.123\,02)\varepsilon + (0.620\,25 + i0.061\,12)\varepsilon^2.$$

The poor convergence of the  $\varepsilon$  expansion is already shown in the two-loop order values of the biconical FP  $\mathcal{B}$  in  $d=3$ . This FP does not satisfy the criterion

$$\Delta^* = u_{\parallel}^* u_{\perp}^* - u_{\times}^{*2} > 0 \quad (39)$$

for describing tetracritical behavior as in zero-loop order [see Eq. (5.12) in Ref. [4] and the discussion in Sec. VII below].

From the structure of the  $\beta$  functions one can derive exact values of some of the stability exponents, as shown in Table I. There, by  $\omega^{\mathcal{H}(n)}$  we denote the usual stability exponent of the  $O(n)$  model. The rest of the exponents are defined at the appropriate FPs by

$$\omega_2^{\mathcal{H}(n_{\perp})} = \partial\beta_{u_{\times}}/\partial u_{\times}|_{\mathcal{H}(n_{\perp})}, \quad (40)$$

$$\omega_2^{\mathcal{H}(n_{\parallel})} = \partial\beta_{u_{\times}}/\partial u_{\times}|_{\mathcal{H}(n_{\parallel})}, \quad (41)$$

$$\omega_2^{\mathcal{D}} = \partial\beta_{u_{\times}}/\partial u_{\times}|_{\mathcal{D}}. \quad (42)$$

To find the stability exponents in the FPs  $\mathcal{H}(n_{\perp}+n_{\parallel})$  and  $\mathcal{B}$  one should solve the appropriate secular equation.

One can see from Table I that three FPs  $\mathcal{G}$ ,  $\mathcal{H}(n_{\perp})$ , and  $\mathcal{H}(n_{\parallel})$  are never stable for  $d < 4$ . However, as we will see below, the stability of the other three FPs for  $d < 4$  depends on the values of  $n_{\perp}$  and  $n_{\parallel}$ . As long as two stability exponents of the decoupling FP  $\mathcal{D}$  are always positive,  $\omega^{\mathcal{H}(n_{\perp})}, \omega^{\mathcal{H}(n_{\parallel})} > 0$ , the stability of  $\mathcal{D}$  is defined by the sign of the exponent  $\omega_2^{\mathcal{D}}$ . Therefore, the equation for the marginal dimension line in the  $n_{\perp}$ - $n_{\parallel}$  plane reads

$$\partial\beta_{u_{\times}}/\partial u_{\times}|_{\mathcal{D}} = 0. \quad (43)$$

Equation (43) defines a curve  $n_{\perp}^{\mathcal{D}}(n_{\parallel})$  [or, equivalently,  $n_{\parallel}^{\mathcal{D}}(n_{\perp})$ ] that borders a region of  $n_{\perp}, n_{\parallel}$  values where the FP  $\mathcal{D}$  is stable. Substituting the second-order result (38) into the function (34), we get from (43)

$$n_{\perp}^{\mathcal{D}}(n_{\parallel}) = \frac{2(16 - n_{\parallel})}{n_{\parallel} + 2} - \frac{48\varepsilon}{n_{\parallel} + 2}. \quad (44)$$

Equation (44) can be inverted and one gets

$$n_{\parallel}^{\mathcal{D}}(n_{\perp}) = \frac{2(16 - n_{\perp})}{n_{\perp} + 2} - \frac{48\varepsilon}{n_{\perp} + 2}. \quad (45)$$

The first term in (44) and (45) coincides with the first-order result of Ref. [4] whereas the second term gives the second-order contribution, which again demonstrates the weakness of the second-order  $\varepsilon$  expansion, since the shift to smaller values of  $n_{\parallel}(n_{\perp})$  in  $d=3$  is drastically overestimated, leading to instability for small values of  $n_{\parallel}$  and/or  $n_{\perp}$ .

Note that the stability properties of the FP  $\mathcal{D}$  can be evaluated on the base of exact scaling arguments [26]. At this FP

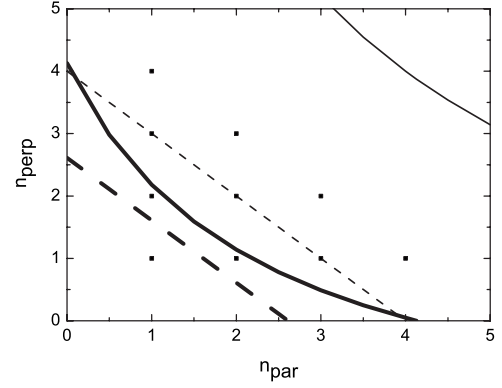


FIG. 1. Regions of different static bicritical behavior in the  $n_{\parallel}$ - $n_{\perp}$  plane ( $\varepsilon=4-d=1$ ), which are defined by the stable FP (from left to right: Heisenberg FP  $\mathcal{H}$ , biconical FP  $\mathcal{B}$ , and decoupling FP  $\mathcal{D}$ ). Shown are the  $\mathcal{H}\mathcal{B}$  stability border line (dashed lines) and  $\mathcal{B}\mathcal{D}$  stability border lines (solid lines), in one-loop order (thin lines) and resummed two-loop order (thick lines). The dots indicate low integer values for OP components. One sees that the borderlines are drastically shifted to smaller values of OP components. Thus in the case  $n_{\parallel}=1$  and  $n_{\perp}=2$  the FP  $\mathcal{B}$  (connected with tetracriticality) is stable in two-loop order, contrary to the one-loop order calculation where the FP  $\mathcal{H}$  (connected with bicriticality) is stable.

the coupling term  $u_{\times}\phi_{\perp}^2\phi_{\parallel}^2$  has a scaling of the product of two energylike operators, the latter having scaling dimensions  $(1-\alpha_{n_{\perp}})/\nu_{n_{\perp}}$  and  $(1-\alpha_{n_{\parallel}})/\nu_{n_{\parallel}}$ , respectively [with  $\alpha_n$  and  $\nu_n$  being the heat capacity and the correlation length critical exponents in the  $O(n)$  universality class]. In turn, this leads to the following formula for the RG dimension  $y_{u_{\times}}$  of the combined operator [5,26]:

$$y_{u_{\times}} = 1/\nu_{n_{\perp}} + 1/\nu_{n_{\parallel}} - d. \quad (46)$$

With available five-loop  $\varepsilon$ -expansion results for the exponents of  $O(n)$  theory [25] the marginal dimensions  $n_{\perp}^{\mathcal{D}}(n_{\parallel})$  [ $n_{\parallel}^{\mathcal{D}}(n_{\perp})$ ] can be estimated.

The first-order result for  $n_{\perp}^{\mathcal{D}}(n_{\parallel})$  is shown in Fig. 1 by a solid line. The FP  $\mathcal{D}$  is stable for the values of  $n_{\perp}, n_{\parallel}$  above this line. Crossing the line, one gets into the region where the biconical FP  $\mathcal{B}$  acquires stability. With further change of  $n_{\perp}, n_{\parallel}$ , its coordinates do change as well, and for certain values of  $n_{\perp}^{\mathcal{H}}(n_{\parallel})$  this FP coincides with the Heisenberg FP  $\mathcal{H}(n_{\parallel}+n_{\perp})$ . Then it loses its stability, and further the FP  $\mathcal{H}(n_{\parallel}+n_{\perp})$  is stable. Therefore, the marginal dimension line  $n_{\perp}^{\mathcal{H}}(n_{\parallel})$  [or  $n_{\parallel}^{\mathcal{H}}(n_{\perp})$  equivalently] can be defined from any of the conditions

$$\beta_{u_{\perp}}(u_{\perp}, u_{\perp}, u_{\perp}) = \beta_{u_{\times}}(u_{\times}, u_{\times}, u_{\times}) = \beta_{u_{\parallel}}(u_{\parallel}, u_{\parallel}, u_{\parallel}) = 0. \quad (47)$$

As long as in the Heisenberg FP  $\mathcal{H}$  the RG functions depend on the sum of field dimensionalities  $n_{\perp}+n_{\parallel}$ , the resulting marginal dimension curve will be of the form  $n_{\perp}^{\mathcal{H}}(n_{\parallel}) = \text{const} - n_{\parallel}$ . Substituting the FP  $\mathcal{H}$  coordinates into the expressions for the  $\beta$  functions (33)–(35) we get the second-order expression for the marginal dimension. By it, we recover the two first terms of the third-order result quoted in Ref. [4] (and obtained from Ref. [27]):

TABLE II. Fixed points and stability exponents of the  $O(1) \oplus O(2)$  model obtained by the Padé-Borel resummation within two loops. Biconical FP  $\mathcal{B}$  is stable.

FP	$u_{\perp}^*$	$u_{\times}^*$	$u_{\parallel}^*$	$\omega_1$	$\omega_2$	$\omega_3$
$\mathcal{G}$	0	0	0	-1	-1	-1
$\mathcal{H}(2)$	1.141	0	0	0.581	-0.461	-1
$\mathcal{H}(1)$	0	0	1.315	-1	-0.552	0.565
$\mathcal{D}$	1.141	0	1.315	0.581	-0.014	0.566
$\mathcal{H}(3)$	1.002	1.002	1.002	0.597	0.407	-0.036
$\mathcal{B}$	1.128	0.301	1.287	0.583	0.554	0.01

$$n_{\perp}^{\mathcal{H}}(n_{\parallel}) = -n_{\parallel} + 4 - 2\varepsilon + c^{\times} \varepsilon^2, \quad (48)$$

with  $c^{\times} = \frac{5}{12}[6\zeta(3) - 1] = 2.5885$ ; or, equivalently,

$$n_{\parallel}^{\mathcal{H}}(n_{\perp}) = -n_{\perp} + 4 - 2\varepsilon + c^{\times} \varepsilon^2. \quad (49)$$

In Fig. 1 the results obtained in the  $\varepsilon$  expansion in first-loop order are shown. Whereas the  $\mathcal{H}\mathcal{B}$  stability border lines lead to an acceptable result, but bad convergence, the  $\mathcal{B}\mathcal{D}$  stability borderlines show unphysical features in the  $\varepsilon$ -expansion. In second order in  $\varepsilon$  the stability borderline for positive values of  $n_{\perp}$  lies at negative values of  $n_{\parallel}$ , meaning that the decoupling fixed point is stable in the whole region shown. The second-order  $\varepsilon$  expansion results do not lead to reliable results being estimated naively. Therefore, below we will reanalyze the RG functions by resumming them in two loops directly for  $\varepsilon=1$ .

The FPs where the parallel and perpendicular systems decouple ( $u_{\times}^*=0$ ) need some comments. The renormalization group procedure used here assumes that the multicritical system is described by one diverging length scale and therefore by one correlation length  $\xi$  and one corresponding critical exponent  $\nu$ . This does not hold for decoupled systems, where two length scales and therefore two correlation lengths  $\xi_{\parallel}$  and  $\xi_{\perp}$  with two different asymptotic exponents  $\nu_{\parallel}$  and  $\nu_{\perp}$  are present. Thus the usual scaling laws with one length scale break down (see the remarks in Refs. [4,28]).

### B. Results from resummation of the two-loop field theoretic functions

Let us pass now to another method of analysis of the RG functions (33)–(35). That is, in the spirit of the fixed-dimension RG approach [17] let us consider the FP equations (37) directly at fixed  $d=3$ . The RG series being divergent, we present the  $\beta$  functions (33)–(35) in the form of a resolvent series and resum them by the Padé-Borel resummation technique as explained in Appendix B. Let us note that such a representation preserves the symmetry properties of the functions. Now, the FP coordinates as well as the marginal dimension lines are evaluated numerically. The lines  $n_{\perp}^{\mathcal{H}}(n_{\parallel})$ ,  $n_{\perp}^{\mathcal{D}}(n_{\parallel})$  are shown in Fig. 1 by solid lines. The FP coordinates for  $n_{\perp}=1, n_{\parallel}=2$  and the stability exponents are given in Table II.

From the resummation at  $n_{\parallel}=1$  and different  $n_{\perp}$  we can follow the changes in the FP values of the fourth-order cou-

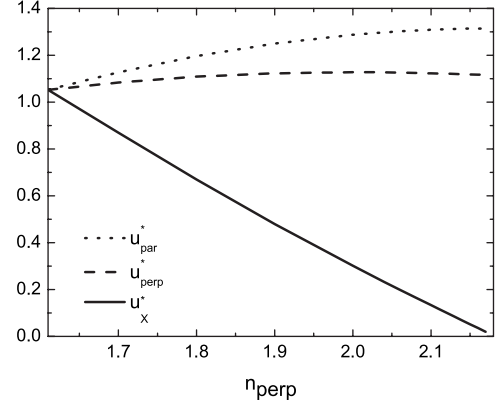


FIG. 2. Dependence of fixed-point values of the static couplings  $u_{\perp}$ ,  $u_{\parallel}$ ,  $u_{\times}$  (in Borel summed two-loop order) on  $n_{\perp}$  for  $n_{\parallel}=1$  in the region of stability of the bicritical fixed point in  $d=3$ .

plings at the biconical FP (see Fig. 2). They start with equal values corresponding to the isotropic Heisenberg FP at the borderline value  $n=1.6$ . The cross coupling between the parallel and perpendicular components decreases to zero at the stability border line to the decoupling FP at  $n_{\perp}(n_{\parallel}=1) = 2.17$ , whereas the other couplings slightly increase.

## VI. IDENTIFICATION OF THE CRITICAL EXPONENTS

The connection between critical exponents and the  $\zeta$  functions can be obtained from the solution of the renormalization group equations for the vertex functions.

### A. Anomalous dimensions $\eta_{\parallel}$ and $\eta_{\perp}$

Considering the vertex functions (A9) at the bicritical point  $\xi_{\perp}^{-2} = \xi_{\parallel}^{-2} = 0$  the renormalization group equation for the  $k$ -dependent functions reads

$$\left( \kappa \frac{\partial}{\partial \kappa} + \sum_{a=\perp, \parallel, \times} \beta_{u_a} \frac{\partial}{\partial u_a} + \frac{1}{2} \sum_{j=1}^N \zeta_{\phi_{\alpha_j}} \right) \Gamma_{\alpha_1 \dots \alpha_N}^{(N,0)}(k, \{u\}, \kappa) = 0. \quad (50)$$

Solving the equation with the method of characteristic equations leads to

$$\Gamma_{\alpha_1 \dots \alpha_N}^{(N,0)}(k, \{u\}, \kappa) = (\kappa l)^{\delta_N} \exp \left( \frac{1}{2} \sum_{j=1}^N \int_1^l \frac{dx}{x} \zeta_{\phi_{\alpha_j}} \right) \times \hat{\Gamma}_{\alpha_1 \dots \alpha_N}^{(N,0)} \left( \frac{k}{\kappa l}, \{u(l)\} \right), \quad (51)$$

where  $\delta_N = N + d - \frac{1}{2}Nd$  is the naive dimension of the vertex functions. The couplings  $\{u(l)\}$  are determined by the flow equations (36). For  $N=2$  the vertex functions represents the  $k$ -dependent inverse susceptibilities in the two subspaces. Equation (51) reduces to

$$\Gamma_{\alpha_i \alpha_i}^{(2,0)}(k, \{u\}, \kappa) = (\kappa l)^2 \exp\left(\int_1^l \frac{dx}{x} \zeta_{\phi_{\alpha_i}}\right) \hat{\Gamma}_{\alpha_i \alpha_i}^{(2,0)}\left(\frac{k}{\kappa l}, \{u(l)\}\right) \quad (52)$$

with the indices (not to be confused with the specific heat exponents below)  $\alpha_i$  equal to  $\perp$  or  $\parallel$ . In the asymptotic region the couplings  $\{u(l)\}$  have nearly reached their fixed-point values  $\{u^*\}$ . The  $\zeta$  function  $\zeta_{\phi_{\alpha_i}}[\{u(x)\}]$  in the exponential factor reduces to the constant  $\zeta_{\phi_{\alpha_i}}(\{u^*\}) \equiv \zeta_{\phi_{\alpha_i}}^*$ . Expression (52) reduces to

$$\Gamma_{\alpha_i \alpha_i}^{(2,0)}(k, \{u\}, \kappa) = \kappa^{2l^{2+\zeta_{\phi_{\alpha_i}}^*}} \hat{\Gamma}_{\alpha_i \alpha_i}^{(2,0)}\left(\frac{k}{\kappa l}, \{u^*\}\right). \quad (53)$$

In order to obtain a finite-amplitude function  $\hat{\Gamma}_{\alpha_i \alpha_i}^{(2,0)}$  we choose the matching condition

$$\frac{k}{\kappa l} = 1, \quad (54)$$

which determines the flow parameter  $l(k)$ . Insertion into (53) leads to

$$\Gamma_{\alpha_i \alpha_i}^{(2,0)}(k, \{u\}, \kappa) = \kappa^2 \left(\frac{k}{\kappa}\right)^{2+\zeta_{\phi_{\alpha_i}}^*} \hat{\Gamma}_{\alpha_i \alpha_i}^{(2,0)}(1, \{u^*\}) \sim k^{2+\zeta_{\phi_{\alpha_i}}^*}. \quad (55)$$

Therefore the asymptotic behavior of the inverse susceptibilities  $\chi_{\alpha_i \alpha_i}^{-1} = \Gamma_{\alpha_i \alpha_i}^{(2,0)}$  is

$$\chi_{\alpha_i \alpha_i}^{-1} \sim k^{2+\zeta_{\phi_{\alpha_i}}^*} \sim k^{2-\eta_{\alpha_i}}. \quad (56)$$

Thus we may identify the two anomalous dimensions

$$\eta_{\alpha_i} = -\zeta_{\phi_{\alpha_i}}^* \quad (57)$$

with  $\alpha_i = \perp, \parallel$ .

### B. Exponents of the susceptibilities $\gamma_{\parallel}$ and $\gamma_{\perp}$

In order to obtain the exponents  $\gamma_{\parallel}$  and  $\gamma_{\perp}$  and their relation to the exponent of the correlation length  $\nu$ , we have to consider the temperature-dependent vertex functions and the corresponding renormalization group equations. There are two methods to include the temperature dependence into the renormalization group equations. The first one is to constitute renormalization group equations for the vertex functions (A6) and derive from the renormalization of the temperature distance  $\Delta \bar{r}$  a relation between the exponents  $\gamma_{\parallel}$  and  $\gamma_{\perp}$  and the corresponding function  $\zeta_r$ . The second one is to constitute a renormalization group equation for the vertex functions (A9) including the temperature dependence by an expansion in  $\phi^2$  insertions. This would lead to a relation of the exponents  $\gamma_{\parallel}$  and  $\gamma_{\perp}$  to the function  $\zeta_{\phi^2}$ . As a consequence of relation (18) one obtains the scaling laws between the exponents  $\gamma_{\parallel}$  and  $\gamma_{\perp}$  and  $\eta_{\parallel}$  and  $\eta_{\perp}$  by including only one exponent  $\nu$  for both correlation lengths (see below). In the following we will consider the first method. The renormalization group equations for the vertex functions (A6) at  $k=0$  read

$$\left(\kappa \frac{\partial}{\partial \kappa} + \sum_{a=\perp, \parallel, \times} \beta_{u_a} \frac{\partial}{\partial u_a} + \Delta \bar{r} \cdot \zeta_{\phi^2} \cdot \frac{\partial}{\partial \Delta \bar{r}} + \frac{1}{2} \sum_{j=1}^N \zeta_{\phi_{\alpha_j}}\right) \Gamma_{\alpha_1 \dots \alpha_N}^{(N,0)}(\{\Delta r\}, \{u\}, \kappa) = 0, \quad (58)$$

where relation (29) has already been used. The matrix  $\zeta_{\phi^2}$  can be diagonalized by the transformation

$$\text{diag}(\zeta_+, \zeta_-) = \mathbf{P}^{-1} \zeta_{\phi^2}^T \mathbf{P} \quad (59)$$

where  $\zeta_+$  and  $\zeta_-$  are the eigenvalues of  $\zeta_{\phi^2}$ , while the matrix  $\mathbf{P}$  is determined by the corresponding eigenvectors. The matrix  $\zeta_{\phi^2}^T$  has the form

$$\zeta_{\phi^2}^T = \frac{1}{6} \begin{pmatrix} V_{\perp} & n_{\parallel} u_{\times} C \\ n_{\perp} u_{\times} C & V_{\parallel} \end{pmatrix}. \quad (60)$$

The functions  $V_{\perp} = V_{\perp}(\{u\})$ ,  $V_{\parallel} = V_{\parallel}(\{u\})$ , and  $C = C(\{u\})$  may contain all orders of loop expansion. The two-loop expressions have been given in (23)–(28). The eigenvalues of this matrix read

$$\zeta_{\pm} = \frac{1}{12} (\Sigma \pm W), \quad (61)$$

where we have introduced the square root

$$W = \sqrt{\Delta^2 + 4n_{\perp} n_{\parallel} u_{\times}^2 C^2} \quad (62)$$

and the parameters

$$\Sigma = V_{\perp} + V_{\parallel}, \quad \Delta = V_{\perp} - V_{\parallel}. \quad (63)$$

The corresponding eigenvalues constitute the transformation matrix

$$\mathbf{P} = \begin{pmatrix} 1 & -\frac{2n_{\parallel} u_{\times} C}{\Delta + W} \\ \frac{2n_{\perp} u_{\times} C}{\Delta + W} & 1 \end{pmatrix}, \quad (64)$$

where the first and the second columns are the eigenvectors of  $\zeta_+$  and  $\zeta_-$ . The explicit appearance of the parameters (62) and (63) in the matrix (64) may differ by using the relation

$$(\Delta + W)(\Delta - W) = -4n_{\perp} n_{\parallel} u_{\times}^2 C^2. \quad (65)$$

For special cases the eigenvalues and the eigenvectors may simplify considerably.

(i) In the case of the decoupled system, where  $u_{\times} = 0$ , a decay into two isolated isotropic subsystems with order parameter dimensions  $n_{\perp}$  and  $n_{\parallel}$  occurs. The matrix (64) reduces to the unit matrix and the eigenvalues  $\zeta_+ = V_{\perp}/6 = \zeta_{\phi^2}^{(n_{\perp})}$  and  $\zeta_- = V_{\parallel}/6 = \zeta_{\phi^2}^{(n_{\parallel})}$  are the corresponding isotropic  $\zeta$  functions of the two subsystems.

(ii) In the case of the isotropic Heisenberg system, i.e.,  $u_{\perp} = u_{\parallel} = u_{\times} = u$ , the matrix (64) reduces to

$$\mathbf{P} = \begin{pmatrix} 1 & -n_{\parallel}/n_{\perp} \\ 1 & 1 \end{pmatrix}, \quad (66)$$

which is independent of  $u$  also in higher-order perturbation expansion. The first eigenvector  $\vec{g}_+^T = (1, 1)$ , which corre-



sponds to  $\zeta_+$ , points in a  $45^\circ$  direction from the bicritical point in the  $\Delta r_\perp$ - $\Delta r_\parallel$  plane, while the second eigenvector  $\vec{g}_- = (-n_\parallel/n_\perp, 1)$  lies in some sense tangentially to it. The eigenvalues in two-loop order are

$$\zeta_+ = \frac{n_\perp + n_\parallel + 2}{6} u \left( 1 - \frac{5}{12} u \right) = \zeta_{\phi^2}^{(n_\perp + n_\parallel)}, \quad (67)$$

$$\zeta_- = \frac{u}{3} \left( 1 - \frac{n_\perp + n_\parallel + 10}{24} u \right), \quad (68)$$

from which one can see that  $\zeta_+$  reproduces in this case the corresponding  $\zeta$  function of an isotropic  $n_\perp + n_\parallel$  component Heisenberg system. The eigenvalues and the directions of the eigenvectors imply that obviously  $\zeta_+$  defines an exponent  $\nu$ , while the other eigenvalue  $\zeta_-$  is connected with a crossover exponent.

Diagonalizing  $\zeta_{\phi^2}$  and introducing transformed temperature distances

$$\vec{r}_\pm \equiv \begin{pmatrix} r_+ \\ r_- \end{pmatrix} = \mathbf{P}^{-1} \cdot \Delta \vec{r} \quad (69)$$

in Eq. (58) we obtain the renormalization group equation

$$\left( \kappa \frac{\partial}{\partial \kappa} + \sum_{a=\perp, \parallel, \times} \beta_{u_a} \frac{\partial}{\partial u_a} + \zeta_+ r_+ \frac{\partial}{\partial r_+} + \zeta_- r_- \frac{\partial}{\partial r_-} + \frac{1}{2} \sum_{j=1}^N \zeta_{\phi_{\alpha_j}} \right) \Gamma_{\alpha_1 \dots \alpha_N}^{(N,0)}(r_+, r_-, \{u\}, \kappa) = 0. \quad (70)$$

The solution of this equation is

$$\Gamma_{\alpha_1 \dots \alpha_N}^{(N,0)}(r_+, r_-, \{u\}, \kappa) = (\kappa l)^{\delta_N} \exp \left( \frac{1}{2} \sum_{j=1}^N \int_1^l \frac{dx}{x} \zeta_{\phi_{\alpha_j}} \right) \times \hat{\Gamma}_{\alpha_1 \dots \alpha_N}^{(N,0)} \left( \frac{r_+(l)}{(\kappa l)^2}, \frac{r_-(l)}{(\kappa l)^2}, \{u(l)\} \right), \quad (71)$$

where the transformed temperature distances satisfy the flow equations

$$l \frac{dr_\pm}{dl} = r_\pm \zeta_\pm(\{u\}). \quad (72)$$

Considering the solution (71) in the asymptotic region  $\{u\} = \{u^*\}$ , we obtain for  $N=2$

$$\Gamma_{\alpha_i \alpha_j}^{(2,0)}(r_+, r_-, \{u\}, \kappa) = \kappa^2 l^{2+\zeta_{\phi_{\alpha_i}}} \hat{\Gamma}_{\alpha_i \alpha_j}^{(2,0)} \left( \frac{r_+(l)}{(\kappa l)^2}, \frac{r_-(l)}{(\kappa l)^2}, \{u^*\} \right). \quad (73)$$

As discussed above,  $r_+$  is the temperature distance to the bicritical point; thus the matching condition

$$\frac{r_+(l)}{(\kappa l)^2} = 1 \quad (74)$$

defines the flow parameter  $l(r_+)$  as a function of temperature. In the asymptotic region the solution of Eq. (72) is

$$r_\pm(l) = r_\pm l^{\zeta_\pm^*}. \quad (75)$$

From (74) we obtain therefore

$$l = \left( \frac{r_+}{\kappa^2} \right)^{1/(2-\zeta_+^*)}. \quad (76)$$

Insertion into (73) leads to the asymptotic expression

$$\Gamma_{\alpha_i \alpha_j}^{(2,0)}(r_+, r_-, \{u\}, \kappa) = \kappa^2 \left( \frac{r_+}{\kappa^2} \right)^{\gamma_{\alpha_i}} \hat{\Gamma}_{\alpha_i \alpha_j}^{(2,0)} \left( 1, \frac{r_- \kappa^2}{(r_+ \kappa^2)^\phi}, \{u^*\} \right) \quad (77)$$

of the inverse order parameter susceptibility, and we may identify the exponent  $\gamma_{\alpha_i}$  and the crossover exponent  $\phi$  as

$$\gamma_{\alpha_i} = \frac{2 + \zeta_{\phi_{\alpha_i}}^*}{2 - \zeta_+^*}, \quad \phi = \frac{2 - \zeta_-^*}{2 - \zeta_+^*}. \quad (78)$$

Introducing  $\eta_{\alpha_i}$  from (57) into the first relation, one can write

$$\gamma_{\alpha_i} = \frac{2 - \eta_{\alpha_i}}{2 - \zeta_+^*} = \nu(2 - \eta_{\alpha_i}), \quad (79)$$

which obviously leads to the exponent

$$\nu^{-1} = 2 - \zeta_+^* \equiv \nu_-^{-1} \quad (80)$$

of the correlation length. Although two exponents  $\eta_{\alpha_i}$  ( $\alpha_i = \perp, \parallel$ ), and as a consequence, two exponents  $\gamma_{\alpha_i}$ , have been obtained, only one exponent  $\nu$  describes the multicritical behavior. This reflects the fact that the anisotropy is present only in the order parameter component space, but not in the coordinate space. Only a single diverging length scale is present in the system in our case; for a discussion when two length scales are present, see Ref. [28]. For the discussion in Sec. VI D it is convenient to define the exponent

$$\nu_-^{-1} \equiv 2 - \zeta_-^* \quad (81)$$

quite analogous to (80). The crossover exponent in (78) can then be written as

$$\phi = \frac{\nu_+}{\nu_-}. \quad (82)$$

### C. Exponent of the specific heat $\alpha$

Within the Ginzburg-Landau-Wilson model the specific heat is proportional to the  $\phi^2 - \phi^2$  correlation function, which is the negative vertex function  $\Gamma^{(0,2)}$ . Therefore we have to consider the solutions of the renormalization group equations for  $\Gamma_{;\beta_1 \beta_2}^{(0,2)}$  defined in (13) in order to obtain a theoretical expression for the exponent  $\alpha$ . Considering the functions  $\Gamma_{;\beta_1 \beta_2}^{(0,2)}$  as a symmetric matrix

$$\Gamma^{(0,2)} = \begin{pmatrix} \Gamma_{;\perp \perp}^{(0,2)} & \Gamma_{;\perp \parallel}^{(0,2)} \\ \Gamma_{;\perp \parallel}^{(0,2)} & \Gamma_{;\parallel \parallel}^{(0,2)} \end{pmatrix}, \quad (83)$$

the renormalization group equation reads

$$\left( \kappa \frac{\partial}{\partial \kappa} + \sum_{a=\perp, \parallel, \times} \beta_{u_a} \frac{\partial}{\partial u_a} + \Delta \vec{r} \cdot \zeta_{\phi^2} \cdot \frac{\partial}{\partial \Delta \vec{r}} - \varepsilon \right) \Gamma^{(0,2)} + \zeta_{\phi^2} \cdot \Gamma^{(0,2)} + \Gamma^{(0,2)} \cdot \zeta_{\phi^2}^T = -\mathbf{B}_{\phi^2}, \quad (84)$$

where the vertex function is taken at  $k=0$ , i.e.,  $\Gamma^{(0,2)} = \Gamma^{(0,2)}(\{\Delta r\}, \{u\}, \kappa)$ . The term  $-\varepsilon$  is the naive dimension of the vertex function and it appears explicitly because  $\Gamma^{(0,2)}$  has been introduced as a dimensionless quantity in (13). Introducing the diagonalized  $\zeta$  functions (59) and the transformed temperature distances (69), Eq. (84) can be rewritten as

$$\left( \kappa \frac{\partial}{\partial \kappa} + \sum_{a=\perp, \parallel, \times} \beta_{u_a} \frac{\partial}{\partial u_a} + \zeta_{+r_+} \frac{\partial}{\partial r_+} + \zeta_{-r_-} \frac{\partial}{\partial r_-} - \varepsilon \right) \Gamma_{\pm}^{(0,2)} + 2 \text{diag}(\zeta_{+}, \zeta_{-}) \cdot \Gamma_{\pm}^{(0,2)} = -\mathbf{B}_{\phi^2}^{(\pm)}. \quad (85)$$

The transformed vertex functions are

$$\Gamma_{\pm}^{(0,2)} \equiv \begin{pmatrix} \Gamma_{++}^{(0,2)} & \Gamma_{+-}^{(0,2)} \\ \Gamma_{-+}^{(0,2)} & \Gamma_{--}^{(0,2)} \end{pmatrix} = \mathbf{P}^T \cdot \Gamma^{(0,2)} \cdot \mathbf{P}. \quad (86)$$

Quite analogously,  $\mathbf{B}_{\phi^2}^{(\pm)} = \mathbf{P}^T \cdot \mathbf{B}_{\phi^2} \cdot \mathbf{P}$ . Applying the matrix (66) from the isotropic case one obtains  $\Gamma_{++}^{(0,2)} = \Gamma_{\perp\perp}^{(0,2)} + 2\Gamma_{\perp\parallel}^{(0,2)} + \Gamma_{\parallel\parallel}^{(0,2)}$ , which is the specific heat in the isotropic Heisenberg model. Thus in the present case the specific heat is obviously proportional to  $\Gamma_{++}^{(0,2)}$ . The corresponding renormalization group equation is

$$\left( \kappa \frac{\partial}{\partial \kappa} + \sum_{a=\perp, \parallel, \times} \beta_{u_a} \frac{\partial}{\partial u_a} + \zeta_{+r_+} \frac{\partial}{\partial r_+} + \zeta_{-r_-} \frac{\partial}{\partial r_-} + 2\zeta_{+} - \varepsilon \right) \Gamma_{++}^{(0,2)} = -\mathbf{B}_{\phi^2}^{(++)} \quad (87)$$

with the solution

$$\begin{aligned} \Gamma_{++}^{(0,2)}(r_+, r_-, \{u\}, \kappa) &= \exp\left( \int_1^l \frac{dx}{x} (2\zeta_{+} - \varepsilon) \right) \\ &\quad \times \hat{\Gamma}_{++}^{(0,2)}\left( \frac{r_+(l)}{(\kappa l)^2}, \frac{r_-(l)}{(\kappa l)^2}, \{u(l)\} \right) \\ &\quad + \int_1^l \frac{dx}{x} \\ &\quad \times \mathbf{B}_{\phi^2}^{(++)}(\{u(l)\}) \exp\left( \int_1^x \frac{dx'}{x'} (2\zeta_{+} - \varepsilon) \right). \end{aligned} \quad (88)$$

Using (74)–(76) the expression reduces in the asymptotic region to

$$\Gamma_{++}^{(0,2)}(r_+, r_-, \{u\}, \kappa) = \left( \frac{r_+}{\kappa^2} \right)^{-\alpha} \left[ \hat{\Gamma}_{++}^{(0,2)}\left( 1, \frac{r_-/\kappa^2}{(r_+/\kappa^2)^{1/\phi}}, \{u^*\} \right) + \frac{\mathbf{B}_{\phi^2}^{(++)}(\{u^*\})}{2\zeta_{+}^* - \varepsilon} \right], \quad (89)$$

where  $\alpha$  is given by

$$\alpha = \frac{\varepsilon - 2\zeta_{+}^*}{2 - \zeta_{+}^*} = 2 - \frac{d}{2 - \zeta_{+}^*} = 2 - d\nu. \quad (90)$$

In the last equality we have used Eq. (80). Thus the hyperscaling relation has been derived from the renormalization group equation for the specific heat.

#### D. Numerical estimates for asymptotic critical exponents and scaling

The results for marginal dimensions presented above in Sec. V give evidence that for the physically relevant case  $n_{\parallel}=1$ ,  $n_{\perp}=2$  the biconical FP  $\mathcal{B}$  is stable. Substituting the  $\varepsilon$  expansion for the biconical FP  $\mathcal{B}$  we recover the results presented in Ref. [5]. Although the second order of perturbation theory is known as an optimal truncation for the  $\varepsilon$  expansion, in our case the values for the exponents are not reliable. Resummation of the  $\varepsilon$  expansion in this order does not make much sense.

Therefore we choose another way to estimate the numerical values of the exponents making use of the fixed  $d$  expansions. There, we proceed as follows. First, based on the two-loop expressions (23)–(26) for the matrix  $[\zeta_{\phi^2}]_{ij}(\{u\})$  (22) we find its eigenvalues as expansions in renormalized couplings. In turn, the exponents  $\nu_+$ ,  $\nu_-$  are expressed in terms of the corresponding eigenvalues as series in renormalized couplings as well. Corresponding series are found also for the magnetic susceptibility exponents. The series are then resummed (as described in Appendix B) and evaluated at the FPs. Numerical results of the exponents  $\nu_+$ ,  $\nu_-$ ,  $\gamma_{\parallel}$ , and  $\gamma_{\perp}$  obtained by such evaluation are given in Table III in the (stable) biconical FP  $\mathcal{B}$  and, for comparison, in the (unstable) Heisenberg FP  $\mathcal{H}$ . The expressions for the exponents  $\eta_{\perp}$  and  $\eta_{\parallel}$  are too short to be resummed. Therefore their numerical values are found from the familiar scaling relations  $\eta_{\parallel}=2 - \gamma_{\parallel}/\nu_+$ ,  $\eta_{\perp}=2 - \gamma_{\perp}/\nu_+$  using resummed values of  $\gamma$  and  $\nu$ . For the decoupling FP one has to modify the scaling relations according to the statements above and has to use  $\eta_{\parallel}=2 - \gamma_{\parallel}/\nu_-$ ,  $\eta_{\perp}=2 - \gamma_{\perp}/\nu_+$ . Note that, within the accuracy of calculations, the results for the exponents that correspond to parallel and perpendicular fields do not differ (the difference shows up within the fourth digit). The overall agreement with the five loop  $\varepsilon$  expansion is very good, especially for the stable biconical FP.

### VII. FLOW EQUATIONS AND EFFECTIVE EXPONENTS

The resummation of the  $\beta$  function has the big advantage of finding the fixed-point values and asymptotic exponents but in addition the flow of the couplings from their background values to their FP values. The flow is important for the crossover behavior but also for the discussion of the asymptotic multicritical behavior of physical representatives of such systems with different background values of the couplings. Their location in the attraction region of a FP defines the critical behavior.

#### A. Flow of fourth-order couplings

Figure 3 shows the flow lines in the space of the coupling parameters for different initial conditions calculated from the

TABLE III. Critical exponents of the  $O(1) \oplus O(2)$  model obtained by resummation of the two-loop RG series at fixed  $d=3$  in different FPs (first two rows of the table). Our data are compared with the results of Ref. [2] (first-order  $\varepsilon$  expansion), and Refs. [5,29] (resummed fifth-order  $\varepsilon$  expansion). Numbers, shown in italics were obtained via familiar scaling relations.

Reference	FP	$\eta_{\perp}$	$\eta_{\parallel}$	$\gamma_{\perp}$	$\gamma_{\parallel}$	$\nu_{+}$	$\nu_{-}$	$\phi$	$\alpha$
This paper	$\mathcal{B}$	0.037	0.037	1.366	1.366	0.696	0.629	1.144 <sup>a</sup>	-0.088
	$\mathcal{H}(3)$	0.040	0.040	1.411	1.411	0.720	0.564	1.275 <sup>a</sup>	-0.160
Ref. [2]	$\mathcal{B}$	0	0	1.222	1.222	0.611	0.503	1.176	<i>0.167</i>
Ref. [2]	$\mathcal{H}(3)$	0	0	1.227	1.227	0.611	0.505	1.136	<i>0.167</i>
Ref. [5]	$\mathcal{B}$	0.037(5)	0.037(5)	<i>1.37(7)</i>	<i>1.37(7)</i>	0.70(3)	<i>0.56(3)</i>	1.25(1)	<i>-0.10(9)</i>
Ref. [29]	$\mathcal{H}(3)$	0.0375(45)	0.0375(45)	1.382(9)	1.382(9)	0.7045(55)	0.559(17)	<i>1.259(23)</i>	<i>-0.114(17)</i>

<sup>a</sup>Pole in the Padé approximant is present (see Appendix B).

resummed  $\beta$  functions. Mean field theory states a criterion [1] which has to be satisfied by the fourth-order couplings for the existence of a tetracritical point; it reads

$$\Delta = u_{\parallel}u_{\perp} - u_{\times}^2 > 0. \quad (91)$$

The flow equations show that  $\Delta$  is not an invariant surface of the flow. However, it contains several separatrices with the corresponding fixed points: the decoupling FPs with  $u_{\times}^* = 0$  ( $\mathcal{G}, \mathcal{H}(1), \mathcal{H}(2), \mathcal{D}$ ) and the Heisenberg FP  $\mathcal{H}(3)$ . Therefore in the region shown in Fig. 1 the mean field condition  $\Delta = 0$  represents quite well the surface [called the mean field surface (MFS)] separating the attraction region of the biconical FP  $\mathcal{B}$  and the region of runaway flows.

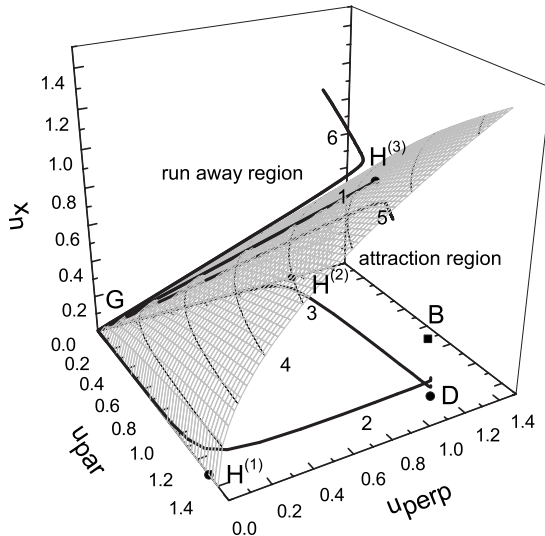


FIG. 3. Resummed flow for different initial conditions. The unstable FPs are shown as filled spheres, the stable biconical FPs filled cubes. In order to show the crossover, the initial values of couplings are chosen accordingly. Due to the small transient exponent present, the stable fixed point is not reached for the small value of the flow parameter chosen. The fixed points are connected by separatrices defining the surface which encloses the attraction region. It is slightly different from the MFS surface shown (for further details see text). The initial values of flow 6 are outside the attraction regions. The flow parameter is changed in the interval  $-40 \leq \ln l \leq 0$ .

Thus one can draw the following conclusions. A system with initial conditions  $\Delta < 0$  lies outside the attraction region of the stable FP and its runaway flow indicates that a first-order transition is expected. One would conclude that the multicritical point is a triple point. Systems with initial conditions where roughly  $\Delta = 0$  would flow to the Heisenberg FP  $\mathcal{H}(3)$ , indicating that the multicritical point is a bicritical point. Then finally if the initial conditions are such that  $\Delta > 0$  the biconical FP  $\mathcal{B}$  is reached and the multicritical point is a tetracritical point. In this way the three scenarios sketched in Ref. [5] are realized. The important and open point is to connect the initial conditions of the field theoretic flow equations to the interaction parameters in the appropriate spin Hamiltonian containing the anisotropic interactions defining the antiferromagnetic system.

## B. Effective exponents

Having available the solutions of the flow equations, one can define the effective exponents by evaluating the field theoretic  $\zeta$  functions at the values of the couplings given by the flow according to the definitions of the exponents in Eqs. (57) and (80). We substitute the couplings obtained from the resummed flow equations into the resummed  $\zeta$  functions appearing in the expressions for exponents. In this way the effective exponents become functions of the flow parameter  $l$ , e.g.,

$$\nu_{+\text{eff}}^{-1}(l) = 2 - \zeta_{+}(u_{\parallel}(l), u_{\perp}(l), u_{\times}(l)) = \nu_{\text{eff}}^{-1}(l),$$

$$\nu_{-\text{eff}}^{-1}(l) = 2 - \zeta_{-}(u_{\parallel}(l), u_{\perp}(l), u_{\times}(l)). \quad (92)$$

The effective crossover exponent  $\phi_{\text{eff}}$  follows from Eq. (82) as

$$\phi_{\text{eff}}(l) = \frac{\nu_{+\text{eff}}(l)}{\nu_{-\text{eff}}(l)}. \quad (93)$$

Results for the exponents are shown in Figs. 4–6.

The two exponents of the parallel and perpendicular OP susceptibilities are almost equal even in the nonasymptotic region, but might be quite different from the asymptotic value. In particular, due to the slow transient present, the values for the flows 1–3 are smaller than the expected asymptotic values. The same holds for the effective exponent of the correlation length  $\nu_{\text{eff}}$ . The flow 6, which does not

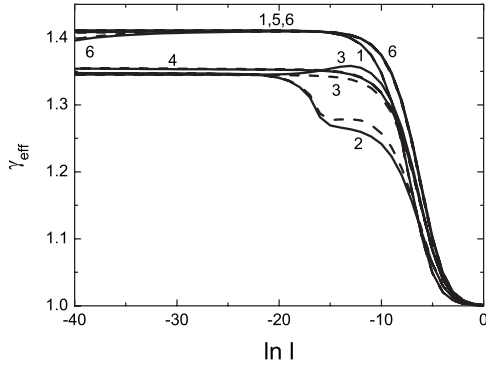


FIG. 4. Effective exponent  $\gamma_{\parallel}$  (solid lines) and  $\gamma_{\perp}$  (dashed lines) for the initial conditions of flows shown in Fig. 3.

reach a finite fixed point, lies within the expected values. The formal decrease of the effective exponents to unphysical negative values is due to the flow to infinite values of the couplings.

### VIII. CONCLUSION AND OUTLOOK

We have shown that the two-loop order perturbation theory together with appropriate resummation techniques is sufficient to calculate the multicritical behavior appearing in systems with  $O(n_{\parallel}) \oplus O(n_{\perp})$  symmetry at fixed dimension. The advantage of such a procedure lies in the accessibility of the corresponding flow equations, which allow a discussion of attraction regions and effective (crossover) critical behavior. We confirmed the shift of the one-loop stability border lines, with the consequence that the multicritical behavior for the case  $n_{\parallel}=1$  and  $n_{\perp}=2$  is characterized by the stable biconical fixed point and not by the Heisenberg fixed point. The discussion of the attraction region of this fixed point leads to the possibility of different phase diagrams depending on the nonuniversal initial parameters entering the flow equations.

In a next step the results will be used to reconsider the dynamical critical behavior of the pure relaxational dynamics [30] of these systems. For the bicritical dynamics of an antiferromagnet in an external magnetic field an extension of the above mentioned model is necessary since, besides the OP, conserved densities have to be taken into account. In

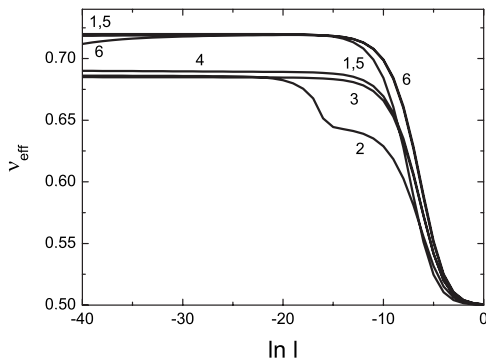


FIG. 5. Effective exponents  $\nu$  for the initial conditions of flows shown in Fig. 3.

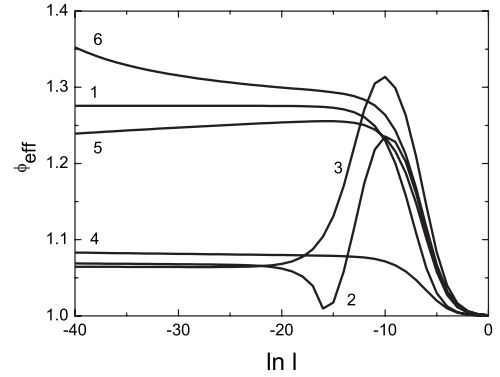


FIG. 6. Effective exponents  $\phi$  for the initial conditions of flows shown in Fig. 3.

statics these couplings appear only up to second-order terms and can be integrated out. In dynamics they lead to a coupling of the two dynamic equations. A complete description of the dynamical multicritical behavior has not been given in two-loop order so far. Finally, mode coupling terms have to be taken into account up to two-loop order.

*Note added in proof.* The model we consider here was analyzed by the massive RG scheme in a resummed two loop order in Ref. [35]. Although the shift of the stability border lines agrees qualitatively with our results there are quantitative differences to our two loop calculation within the minimal subtraction scheme and the five loop  $\epsilon$  expansion of Ref. [5]. Moreover, only the asymptotic properties were analyzed there. We thank A. Fedorenko for bringing this important publication to our attention.

### ACKNOWLEDGMENTS

We thank W. Selke for useful discussions. This work was supported by the Fonds zur Förderung der wissenschaftlichen Forschung under Project No. P19583-N20.

### APPENDIX A: VERTEX FUNCTIONS AND PERTURBATION EXPANSION

With the static functional (3) the vertex functions

$$\overset{\circ}{\Gamma}_{\alpha_1 \dots \alpha_N; \beta_1 \dots \beta_L}^{(N,L)}(\{\hat{r}\}, \{\hat{u}\}, k) \quad (\text{A1})$$

can be calculated in a definite loop order by collecting all one-particle-irreducible contributions.  $N$  and  $L$  are the total numbers of  $\phi$  and  $\phi^2$  insertions and the indices  $\alpha_i$  and  $\beta_j$  indicate if the corresponding insertion is of type  $\perp$  or  $\parallel$ .  $\{\hat{r}\} \equiv \hat{r}_{\perp}, \hat{r}_{\parallel}$  and  $\{\hat{u}\} \equiv \hat{u}_{\perp}, \hat{u}_{\times}, \hat{u}_{\parallel}$  act as placeholders for the two temperature distances and three fourth-order couplings. Between the lower critical dimension  $d_u=2$  and the upper critical dimension  $d_c=4$ , the vertex functions (A1) also contain singularities at  $d=3$ . They have their origin in a nonanalytical shift of the critical temperature as a function of the four-point couplings (for more details see the third reference in Ref. [17]). In order to remove them, two parameters  $\hat{r}_{\perp c}$  and  $\hat{r}_{\parallel c}$  are introduced. They are determined by



$$\mathring{\Gamma}_{\perp\perp}^{(2,0)}(\{0\},\{\hat{u}\},0) = \mathring{r}_{\perp c}, \quad (\text{A2})$$

$$\mathring{\Gamma}_{\parallel\parallel}^{(2,0)}(\{0\},\{\hat{u}\},0) = \mathring{r}_{\parallel c}. \quad (\text{A3})$$

This defines the functions  $\mathring{r}_{\perp c}(\{\hat{u}\})$  and  $\mathring{r}_{\parallel c}(\{\hat{u}\})$ . Introducing

$$\Delta\mathring{r}_{\perp} = \mathring{r}_{\perp} - \mathring{r}_{\perp c}(\{\hat{u}\}), \quad (\text{A4})$$

$$\Delta\mathring{r}_{\parallel} = \mathring{r}_{\parallel} - \mathring{r}_{\parallel c}(\{\hat{u}\}) \quad (\text{A5})$$

and rewriting the expressions for (A1) leads to vertex functions

$$\mathring{\Gamma}_{\alpha_1 \dots \alpha_N; \beta_1 \dots \beta_L}^{(N,L)}(\{\Delta\mathring{r}\},\{\hat{u}\},k). \quad (\text{A6})$$

For dimensions larger than 2, all perturbation contributions now have only singularities at least at  $d=4$ . Further, it may be convenient to introduce the correlation length instead of the temperature distance. In the present case, two correlation lengths

$$\xi_{\perp}^2(\{\Delta\mathring{r}\},\{\hat{u}\}) = \left. \frac{\partial}{\partial k^2} \ln \mathring{\Gamma}_{\perp\perp}^{(2,0)}(\{\Delta\mathring{r}\},\{\hat{u}\},k) \right|_{k=0}, \quad (\text{A7})$$

$$\xi_{\parallel}^2(\{\Delta\mathring{r}\},\{\hat{u}\}) = \left. \frac{\partial}{\partial k^2} \ln \mathring{\Gamma}_{\parallel\parallel}^{(2,0)}(\{\Delta\mathring{r}\},\{\hat{u}\},k) \right|_{k=0} \quad (\text{A8})$$

have to be introduced. Inserting the reversed equations  $\Delta\mathring{r}_{\perp} = \Delta\mathring{r}_{\perp}(\{\xi\},\{\hat{u}\})$  and  $\Delta\mathring{r}_{\parallel} = \Delta\mathring{r}_{\parallel}(\{\xi\},\{\hat{u}\})$  into (A6) leads to functions

$$\mathring{\Gamma}_{\alpha_1 \dots \alpha_N; \beta_1 \dots \beta_L}^{(N,L)}(\{\xi\},\{\hat{u}\},k). \quad (\text{A9})$$

Introduction of the correlation lengths in the vertex functions is a resummation procedure which removes the expanded contributions of the correlation length from the vertex functions. This leads to expressions that are simplified considerably. Moreover, this is true for the calculations in dynamic models (see, for instance, Sec. II). Within statics the two-point functions reveal then the general structure

$$\mathring{\Gamma}_{\perp\perp}^{(2,0)}(\{\xi\},\{\hat{u}\},k) = \frac{\mathring{f}_{\perp}(\{\xi\},\{\hat{u}\})}{\xi_{\perp}^2} + k^2 \mathring{g}_{\perp}(\{\xi\},\{\hat{u}\},k), \quad (\text{A10})$$

$$\mathring{\Gamma}_{\parallel\parallel}^{(2,0)}(\{\xi\},\{\hat{u}\},k) = \frac{\mathring{f}_{\parallel}(\{\xi\},\{\hat{u}\})}{\xi_{\parallel}^2} + k^2 \mathring{g}_{\parallel}(\{\xi\},\{\hat{u}\},k). \quad (\text{A11})$$

In two-loop order the  $k$ -independent function  $\mathring{f}_{\perp}$  is

$$\begin{aligned} \mathring{f}_{\perp}(\{\xi\},\{\hat{u}\}) &= 1 - \frac{n_{\perp} + 2}{18} u_{\perp}^2 \nabla_{k^2} D_3^{\perp\perp}(\xi_{\perp},0) \\ &\quad - \frac{n_{\parallel}}{18} u_{\times}^2 \nabla_{k^2} D_3^{\perp\parallel}(\{\xi\},0), \end{aligned} \quad (\text{A12})$$

where we have introduced the short notation

$$\nabla_{k^2} A(\xi,0) \equiv \left. \frac{\partial A(\xi,k)}{\partial k^2} \right|_{k=0}. \quad (\text{A13})$$

The  $k$ -dependent function  $\mathring{g}_{\perp}$  reads in two-loop order

$$\begin{aligned} \mathring{g}_{\perp}(\{\xi\},\{\hat{u}\},k) &= 1 - \frac{n_{\perp} + 2}{18} u_{\perp}^2 \frac{1}{k^2} [D_3^{\perp\perp}(\xi_{\perp},k) \\ &\quad - D_3^{\perp\perp}(\xi_{\perp},0)] - \frac{n_{\parallel}}{18} u_{\times}^2 \frac{1}{k^2} [D_3^{\perp\parallel}(\{\xi\},k) \\ &\quad - D_3^{\perp\parallel}(\{\xi\},0)]. \end{aligned} \quad (\text{A14})$$

In order to obtain  $\mathring{f}_{\parallel}$  and  $\mathring{g}_{\parallel}$  one only has to interchange  $\perp$  and  $\parallel$ . The two-loop integral  $D_3$  is defined as

$$\begin{aligned} D_3^{\alpha_i \alpha_j \alpha_k}(\{\xi\},k) \\ = \int_{k'} \int_{k''} \frac{1}{(\xi_{\alpha_i}^2 + k'^2)(\xi_{\alpha_j}^2 + k''^2)(\xi_{\alpha_k}^2 + (k+k'+k'')^2)}. \end{aligned} \quad (\text{A15})$$

In the limit  $k \rightarrow 0$  we have

$$\lim_{k \rightarrow 0} \frac{A(\xi,k) - A(\xi,0)}{k^2} = \left. \frac{\partial A(\xi,k)}{\partial k^2} \right|_{k=0} = \nabla_{k^2} A(\xi,0). \quad (\text{A16})$$

Applying the limit to  $\mathring{g}_{\alpha_i}$  [see (A12) and (A14)] one obtains

$$\lim_{k \rightarrow 0} \mathring{g}_{\alpha_i}(\{\xi\},\{\hat{u}\},k) = \mathring{f}_{\alpha_i}(\{\xi\},\{\hat{u}\}), \quad (\text{A17})$$

and the two-point vertex functions reduce in the asymptotic region to

$$\mathring{\Gamma}_{\alpha_i \alpha_i}^{(2,0)}(\{\xi\},\{\hat{u}\},k) \underset{k \rightarrow 0}{\sim} (\xi_{\alpha_i}^2 + k^2) \mathring{f}_{\alpha_i}(\{\xi\},\{\hat{u}\}). \quad (\text{A18})$$

Because the poles do not depend on  $k$ , the two functions  $\mathring{f}_{\alpha_i}$  and  $\mathring{g}_{\alpha_i}$  contain the same pole terms. Thus the two-point functions each may be renormalized by scalar renormalization factors which remove the poles from the functions  $\mathring{f}_{\alpha_i}$ .

## APPENDIX B: RESUMMATION

In this appendix we describe a procedure we use to resum divergent expansions for the two-loop RG functions. Starting from the RG function that has a form of truncated polynomial in renormalized couplings:

$$f(\{u\}) = \sum_{i,j,k=0}^L c_{ijk} u_{\perp}^i u_{\parallel}^j u_{\times}^k \quad (\text{B1})$$

one first represents it in the form of a resolvent series [31] in the variable  $t$ :

$$F(t) = \sum_{i,j,k=0}^L c_{ijk} u_{\perp}^i u_{\parallel}^j u_{\times}^k t^{i+j+k} = \sum_{i=0}^L a_i(\{u\},\{c\}) t^i. \quad (\text{B2})$$

The expansion coefficients  $a_i$  in (B2) explicitly depend on the couplings and coefficient  $c_{ijk}$  (B1). Obviously, for  $t=1$

the function (B2) reproduces the initial RG function (B1):  $F(1)=f(\{u\})$ . Then the function (B2) is resummed as a single variable function and further evaluated at  $t=1$  to recover (B1). To perform the resummation we use the Padé-Borel technique [32]. That is, assuming factorial growth of the expansion coefficients  $a_i$  we define the Borel transform [33] of (B2) by

$$F^B(t) = \sum_{i=0}^L a_i \Gamma(i+1) t^i, \quad (\text{B3})$$

where  $\Gamma(x)$  is the Euler Gamma function. Analytical continuation of the function (B3) is achieved by representing it in a form of a Padé approximant [34]. In our case, working within a two-loop approximation, we use the diagonal  $[1/1]$  Padé approximant

$$F^B(t) \simeq [1/1](t). \quad (\text{B4})$$

Finally, the resummed function is obtained via an inverse Borel transform:

$$F^{\text{res}} = \int_0^\infty [1/1](t) e^{-t}. \quad (\text{B5})$$

The procedure described above was used to analyze the RG flows and exponents. Note, however, that the inverse Borel transform (B5) is well defined, when no poles in the denominator of the Padé approximant (B4) appear. Otherwise one may estimate its principal value. The poles do not appear for a sign-alternating series (as the series for the  $\beta$  functions are). To deal with sign-alternating series during an evaluation of critical exponents, we have resummed the functions  $2-\zeta_\pm$ .

- 
- [1] K.-S. Liu and M. E. Fisher, *J. Low Temp. Phys.* **10**, 655 (1972).
- [2] D. Nelson, J. M. Kosterlitz, and M. E. Fisher, *Phys. Rev. Lett.* **33**, 813 (1974).
- [3] A. Aharony and A. D. Bruce, *Phys. Rev. Lett.* **33**, 427 (1974).
- [4] J. M. Kosterlitz, D. Nelson, and M. E. Fisher, *Phys. Rev. B* **13**, 412 (1976).
- [5] P. Calabrese, A. Pelissetto, and E. Vicari, *Phys. Rev. B* **67**, 054505 (2003).
- [6] For an older review, see Y. Shapira, *Multicritical Phenomena* (Plenum, New York, 1983), p. 35.
- [7] H. Rohrer, *Phys. Rev. Lett.* **34**, 1638 (1975).
- [8] H. Rohrer and Ch. Gerber, *Phys. Rev. Lett.* **38**, 909 (1977).
- [9] A. R. King and H. Rohrer, *Phys. Rev. B* **19**, 5864 (1979).
- [10] R. A. Butera, L. M. Corliss, J. M. Hastings, R. Thomas, and D. Mukamel, *Phys. Rev. B* **24**, 1244 (1981).
- [11] K. Ohgushi and Y. Ueda, *Phys. Rev. Lett.* **95**, 217202 (2005).
- [12] C. C. Becera, N. F. Oliveira, Jr., A. Paduan-Filho, W. Figueiredo, and M. V. P. Souza, *Phys. Rev. B* **38**, 6887 (1988).
- [13] J. A. J. Basten, E. Frikkee, and W. J. M. de Jonge, *Phys. Rev. B* **22**, 1429 (1980).
- [14] M. Holtschneider, W. Selke, and R. Leidl, *Phys. Rev. B* **72**, 064443 (2005).
- [15] W. Selke, M. Holtschneider, R. Leidl, S. Wessel, and G. Bannasch, in *Computer Simulation Studies in Condensed Matter Physics XXI*, edited by D. P. Landau, S. P. Lewis, and H. B. Schüttler (Springer-Verlag, Heidelberg, 2008).
- [16] D. P. Landau and K. Binder, *Phys. Rev. B* **17**, 2328 (1978).
- [17] V. Dohm, *Z. Phys. B: Condens. Matter* **60**, 61 (1985); R. Schloms and V. Dohm, *Europhys. Lett.* **3**, 413 (1987); R. Schloms and V. Dohm, *Nucl. Phys. B* **328**, 639 (1989).
- [18] E. Domany, D. Mukamel, and M. E. Fischer, *Phys. Rev. B* **15**, 5432 (1977).
- [19] S. Murakami and N. Nagaosa, *J. Phys. Soc. Jpn.* **69**, 2395 (2000).
- [20] J. Zinn-Justin, *Quantum Field Theory and Critical Phenomena*, International Series of Monographs on Physics Vol. 92 (Oxford University Press, Oxford, 1996); H. Kleinert and V. Schulte-Frohlinde, *Critical Properties of  $\phi^4$  Theories* (World Scientific, Singapore, 2001).
- [21] V. Dohm, Kernforschungsanlage Jülich Report No. 1578, 1979 (unpublished).
- [22] R. Folk and G. Moser, *J. Phys. A* **39**, R207 (2006).
- [23] This is certainly true for the nondegenerate  $\beta$  functions. A counterexample is given by the random site Ising model. There, a degeneracy of the one-loop  $\beta$  functions leads to appearance of additional FPs on the two-loop level; the latter are proportional to  $\sqrt{\epsilon}$ . For a review, see, e.g., R. Folk, Yu. Holovatch, and T. Yavors'kii, *Usp. Fiz. Nauk* **173**, 175 (2003) [*Phys. Usp.* **46**, 169 (2003)].
- [24] M. Dudka, Yu. Holovatch, and T. Yavors'kii, *J. Phys. A* **37**, 10727 (2004); B. Delamotte, Yu. Holovatch, D. Ivaneyko, D. Mouhanna, and M. Tissier, *J. Stat. Mech.: Theory Exp.* (2008) P03014.
- [25] H. Kleinert, J. Neu, V. Schulte-Frohlinde, K. G. Chetyrkin, and S. A. Larin, *Phys. Lett. B* **272**, 39 (1991); **319**, 545(E) (1993).
- [26] A. Aharony and S. Fishman, *Phys. Rev. Lett.* **37**, 1587 (1976); A. Aharony, *ibid.* **88**, 059703 (2002).
- [27] J. Keyley and D. J. Wallace, *J. Phys. A* **6**, 1667 (1973).
- [28] D. J. Amit and Y. Y. Goldschmidt, *Ann. Phys. (N.Y.)* **114**, 356 (1978).
- [29] R. Guida and J. Zinn-Justin, *J. Phys. A* **31**, (1998) 8103.
- [30] V. Dohm and H.-K. Janssen, *Phys. Rev. Lett.* **39**, 946 (1977).
- [31] P. J. S. Watson, *J. Phys. A* **7**, L167 (1974).
- [32] G. A. Baker, B. G. Nickel, M. S. Green, and D. I. Meiron, *Phys. Rev. Lett.* **36**, 1351 (1976); G. A. Baker, B. G. Nickel, and D. I. Meiron, *Phys. Rev. B* **17**, 1365 (1978).
- [33] G. H. Hardy, *Divergent Series* (Oxford University Press, Oxford, 1948).
- [34] G. A. Baker, Jr. and P. Graves-Morris, *Padé Approximants* (Addison-Wesley: Reading, MA, 1981).
- [35] V. V. Prudnikov, P. V. Prudnikov, and A. A. Fedorenko, *JETP Lett.* **68**, 950 (1998).